Dimensional analysis modeling of spraying operation – Impact of fluid properties and pressure nozzle geometric parameters on the pressure-flow rate relationship

K. Lachin, C. Turchiuli, V. Pistre, G. Cuvelier, S. Mezdour, F. Ducept

Dimensional analysis modeling of spraying operation – Impact of fluid properties and pressure nozzle geometric parameters on the pressure-flow rate relationship

K. LACHIN[a], C. TURCHIULI[a,c], V. PISTRE[a,b], G. CUVELIER[a], S. MEZDOUR[a], F. DUCEPT[a]

[a] Université Paris-Saclay, INRAE, AgroParisTech, SayFood, 91300, Massy, France

[b] TechniProcess, ZI La Muscatelle, 13790 Chateauneuf-Le-Rouge, France

[c] Université Paris-Saclay, IUT d'Orsay, 91400 Orsay, France

Abstract

In food industry, atomization is an essential process as a large range of products are manufactured by spray drying of concentrated solutions. The pressure drop inside the nozzle, and its relation with the flowrate, is of prime importance to size an efficient continuous process. This work thus aims at both studying liquid atomization using pressure nozzles with throttle inserts and proposing a ready-to-use pressure/flowrate correlation from a series of experimental data. Beside the process parameters (flowrate) and fluid parameters (viscosity, density) of prime importance, the geometrical parameters of the nozzle were also accounted for to obtain a generic correlation. Using Newtonian maltodextrin aqueous solutions with viscosity ranging from 1 to 70.10^{-3} Pa.s and eleven nozzle geometries, 264 experiments were performed. Through the use of a dimensionless pressure drop number (Euler number), all the experimental points gathered on a single *Eu** vs. *Re* curve where conventional atomization regimes could be clearly identified. A comprehensive dimensional analysis, relying on the Vashy-Buckingham theorem, was performed. A set of dimensionless correlations, allowing to predict the pressure loss over a wide range of Reynolds number from parameters linked to the fluid, process and nozzle geometry, was then deduced from experimental data.

Keywords

Spray drying, atomization, pressure nozzle, operating diagram, dimensional analysis, pressure drop

1. Introduction

Liquid atomization is a process of prime importance in several industrial sectors for multiple purposes involving the need of fine liquid droplets. It can basically be described as a process which aims at generating droplets from a liquid which is disintegrated in a surrounding gas (Mandato et al., 2012). When it comes to large-scale production, atomization can be found in industries such as (Nasr et al., 2010):

- Pharmaceutics: wet granulation, coating…;
- Paper manufacturing: pulping, moisturizing…;
- Food processing: spray drying, coating, agglomeration…

The atomization stage may have a direct impact on the quality of the end product (as for example, the powder size distribution for spray drying, granulation or agglomeration) and therefore needs to be perfectly understood and controlled. When using nozzles, the parameters influencing the properties of the spray generated mainly falls into three categories:

- The physicochemical properties of the sprayed fluid, including its rheological behavior, surface tension and density;
- The process parameters such as operating pressure, temperature and relative velocity between the fluid and the surrounding air at the nozzle outlet;

- The geometric parameters of the nozzle.

As the main objective of atomization is to generate a fine spray, a substantial amount of the studies on the topic naturally aimed at predicting the average size of the sprayed droplets as a function of some of these parameters (Bayvel and Orzechowski, 1993; Butler Ellis and Tuck, 1999; Hoffmann et al., 2011; Mandato et al., 2012; McCreery and Stoots, 1996). However, the geometric parameters of the nozzle were not systematically taken into account in the establishment of the correlations as it involves a high degree of complexity in the experiments to be performed (several nozzle geometries to be studied and characterized) and in the relations to be found (more coefficients to identify).

Among the diversity of the spray nozzle existing, pressure swirl nozzles are the most commonly used because of their high reliability and low energy requirement, ensuring a good spraying quality (straight droplet size distribution) at small operating costs (Bayvel and Orzechowski, 1993). The main purpose of these devices is to convert pressure into kinetic energy so that the liquid can reach a sufficient velocity when flowing out of the nozzle to ensure the disruption of the film under the shear stress generated. By imposing a swirl motion at some location of the nozzle, the liquid undergoes centrifugal force and leaves the apparatus as a conical sheet (Marchione et al., 2007). When the liquid inlet is tangential to the outlet, the liquid swirl occurs into a chamber before the nozzle exit. In the case the liquid enters axially, the swirl motion is created by an insert with slots designed to this purpose.

When the sizing of a continuous atomization process is required, it may be necessary to know the relationship between the atomized liquid flowrate and the spraying pressure (or pressure drop) ΔP inside the nozzle. This type of relation can practically be of great use for the experimentalist when it comes to estimate the spraying pressure required to proceed a defined flowrate, and determine the minimal flowrate and resulting pressure drop to ensure atomization regime. The relation may be obtained establishing a dimensionless number taking into account the influence of the main parameters. In the process engineering field, pressure-flowrate studies often involve the determination of a discharge coefficient C_D: ratio of the real flowrate (either volumetric or mass) over the theoretical flowrate (ideal conditions) (Lee et al., 2010). This coefficient depends on multiple factors: the shape of the vessel, the liquid properties, the flow regime…. C_D is of prime importance when characterizing the continuous operation of an atomizer (Bayvel and Orzechowski, 1993) as it quantifies the pressure losses due to the passage of the flow through the apparatus. This coefficient can however sometimes be difficult to estimate due to the presence of an air core in the spray: the cross-section area filled by the liquid at the nozzle exit, necessary to estimate C_D, is then different from the orifice area, and this air core has to be somehow predicted to ensure reliable calculations. Due to the wide range of applications of swirl nozzle atomization, a significant amount of experimental studies were performed to investigate the influence of the product and process parameters on the spray angle or air-core diameter (Lee et al., 2010; Halder et al., 2002; Chu et al., 2008; Moon et al., 2009; Alidoost Dafsari et al., 2016; Moon et al., 2010). However few of them focused on the study of axial inlet swirl nozzles with insert and, to the best of the author's knowledge, no extensive study on swirl nozzles with throttle insert was led. Furthermore, solely few correlations taking into account the geometric parameters of the nozzle can be found in the literature for the prediction of the discharge coefficient C_D (Bayvel and Orzechowski, 1993; Jones, 1982; Rizk and Lefebvre, 1985; Ballester and Dopazo, 1994; Jain et al., 2014). And, mainly established for tangential inlet nozzles, these correlations cannot be used for accurate predictions in the case of axial swirl nozzle with throttle inserts, where the geometry can be substantially more complicated

especially knowing that the influence of hydrodynamics was not systematically taken into account in these correlations.

The aim of this paper is therefore to fill in this void and to propose a pressure-flowrate relation for pressure nozzles with throttle inserts. To be as comprehensive as possible in both the product and process parameters and the geometric parameters and hydrodynamics, this relation will be established by the means of a detailed dimensional analysis approach, following the methodology described by Delaplace et al. (Delaplace et al., 2015). The experimental observations combined with the relations obtained will then be discussed and explored to shed some light on the mechanisms at play in this type of device and to propose some guidelines for optimal choice of atomization conditions.

2. Materials and methods

2.1 Sprayed liquids

Aqueous solutions of maltodextrin (MD) of dextrose equivalent (DE) 15 (C.Dry01915, Cargill) were chosen as a model of the liquid feeds usually spray dried in the food industry. Four homogeneous solutions, with a concentration ranging from 0 (pure water) to 47% w/w, were prepared by 5 min mixing at a shear rate of $\dot{\gamma}$ = 100 s^{-1}.

The dynamic viscosity of the solutions at T = 20°C was measured using a Physica MCR 301 rheometer (Anton Paar, Austria). Their Newtonian behavior was confirmed through measurements over a range of shear rate $\dot{\gamma}$ comprised between 100 and 1000 s^{-1}, representative of the shear rates that can be encountered during atomization.

The properties of the four model solutions used in this study are summarized in *Table 1a*.

2.2 Nozzles

Four WDA axial inlet pressure nozzles (Delavan, USA) including a 416 stainless steel distributor and an orifice disc inserted into a brass body were used for the study (*Fig. 1a*). Thanks to rectangular inclined slots carved into the head of the distributor, the liquid (injected axially from the top) exhibits a swirl motion just before going out of the orifice disc, allowing the generation of a hollow-cone spray at the nozzle outlet.

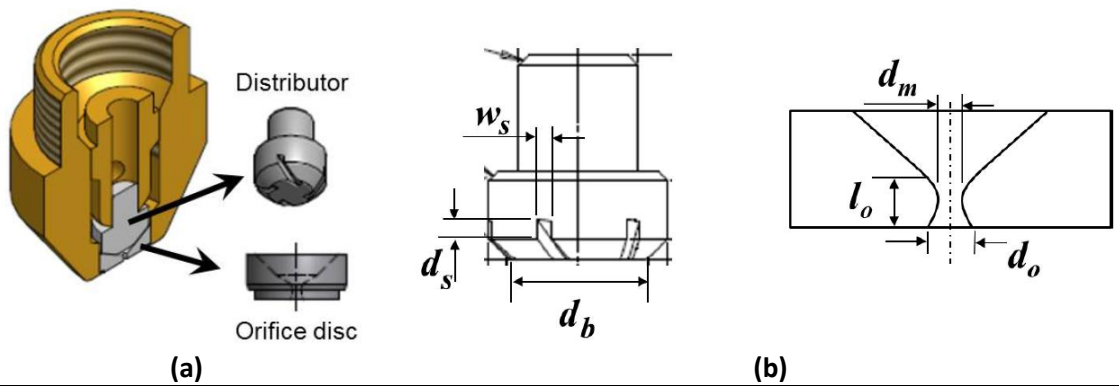

Figure 1: Scheme (a) and geometric parameters (b) of WDA hollow cone pressure nozzles with axial liquid inlet used

As the distributor and orifice disc of each nozzle can be removed, it has been chosen to combine these parts to increase the number of practical nozzle geometries. Over the 16 possible combinations, 11 were selected for the experiments. In order to avoid any confusion, the following nomenclature will be adopted for the designation of the nozzles and recombined nozzles:

- The distributors (inserts) are designated with numbers ranging from *1* to *4*;
- The orifice discs are named with letters from *a* to *d*.

1a, *2b*, *3c* and *4d* thus represent the nozzles as commercialized by the company. For each combination, the main geometric parameters subjected to have an influence on the flow behavior had to be estimated (*Fig. 1b*):

- **Distributor:** the slot width w_s**,** the slot depth d_s, the distributor base diameter d_b, the slot length l_s (not represented) and the number of slots n_s (not represented);
- **Orifice disc:** the orifice minimal diameter d_m, the orifice outlet diameter d_o and the orifice length l_o.

Table 1: Measured value of the maltodextrin solutions properties (20°C) (a) and of the geometric parameters for the different nozzle inserts (b) and orifice discs used (c)

a.

Solution	**1**	**2**	**3**	**4**
MD concentration (kg/kg sol.)	0	0.35	0.42	0.47
Dynamic viscosity μ ($x10^{-3}$ Pa.s)	1	20	40	70
Density ρ ($kg.m^{-3}$)	1000	1100	1150	1155

b.

Insert	**1**	**2**	**3**	**4**
w_s ($x10^{-3}$ m)	0.369	0.239	0.228	0.468
d_s ($x10^{-3}$ m)	0.422	0.387	0.490	0.404
l_s ($x10^{-3}$ m)	1.5	1.5	0.675	0.675
n_s (-)	4	4	6	6
d_b ($x10^{-3}$ m)	3.342	3.342	3.902	3.902

c.

Orifice disc	**a**	**b**	**c**	**d**
d_0 ($x10^{-3}$ m)	0.623	0.942	0.962	0.934
d_m ($x10^{-3}$ m)	0.513	0.523	0.592	0.634
l_o ($x10^{-3}$ m)	0.413	0.322	0.138	0.227

A precise characterization of these dimensions was performed through the use of a profile projector (TESA-Visio 300, TESA, Switzerland). Motorized arms, able to move the geometry along the xyz axes with a precision of 0.5 µm, were used to perform the surface discretization. Through the measurements on two distinct nozzles for each one, it has been established that the measurement accuracy was 5*10-7 m. All the values measured for the different inserts and orifice discs used are gathered in respectively Table 1b and Table 1c.

2.3 Spraying set-up

In order to perform this study, a spraying pilot set-up (TechniProcess, France) was specifically designed (*Fig.2*). It is composed by a thermo-regulated tank equipped with an adequate stirrer (A) (VDA, Milton Roy Mixing, UK), a volumetric tri-piston pump (B) (DOXA B10, Fluidcontrol, Germany), the studied spray nozzle (C) and a tank placed on a scale (D) to collect and weight the sprayed solution.

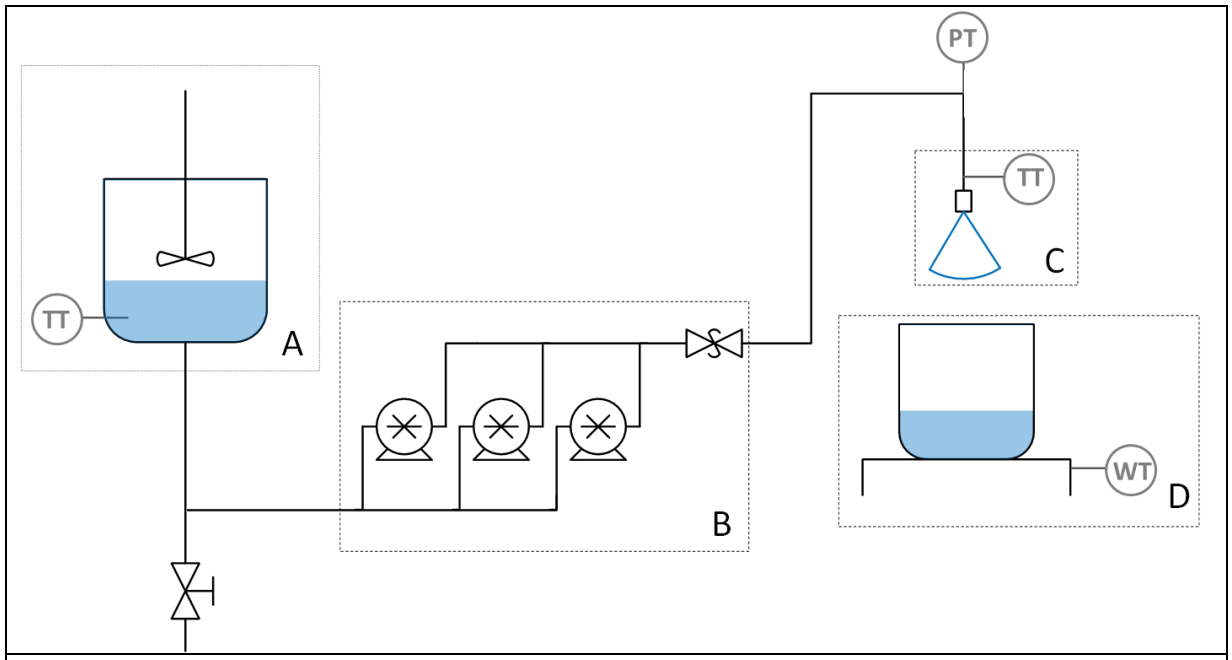

Figure 2: Pilot scale spraying set-up

The temperature of the liquid is measured through the use of thermocouples in the feeding tank and upstream the nozzle. The sprayed liquid mass measurement, performed with a scale (TSI, Timber Productions, France) associated to a timer, allows the determination of the sprayed liquid mass flow rate. For each spraying condition, the liquid flow rate is estimated from the weight measured after a period of 10 minutes. The spraying pressure is measured through a pressure sensor (Midas, JUMO, Germany) located upstream the nozzle. When using tri-piston pumps, the flowrate can be adjusted by either changing the pistons stroke or modifying the operating frequency. It has been chosen for these experiments to maintain the frequency at 50 Hz and to adjust the pistons stroke. For each of the four solutions tested and each of the eleven nozzle geometries considered, between 5 and 10 flow rates in the range 10-50 $L.h^{-1}$ were chosen, corresponding to spraying pressures between 0.5 and 100 bar. Each experiment was repeated: the pressure and flowrate considered in this study are average of values obtained from both experiments. All the 264 experiments performed were supervised through the use of Labview software (Labview, National Instruments, USA).

2.4 Statistical analysis

In the same operating conditions, the difference between the measured flowrate was found to be less than 2%. It was also checked that the pulsating motion of the pump pistons did not have a significant impact on the measured pressure: the variations observed were below 2%.

Coefficients of the dimensional analysis model were determined from the experimental data set using a multiple regression based on the singular value decomposition method. The significance of the obtained coefficients value was successfully checked through a Student test. The variance analysis was also shown to follow a F test. These analyses were performed using the software MATLAB (MATLAB 7.9.0.529, MathWorks, USA).

3. Dimensional analysis

The dimensional analysis performed in this study was established following the guidelines proposed by Delaplace et al. (Delaplace et al., 2015):

- Choice of the target variable and list of the independent parameters/variables related;
- Determination of the dimension of these parameters;
- Use of the Vashy-Buckingham theorem;
- Construction of dimensionless numbers;
- Eventually, reorganization of these numbers.

3.1 Target variable and related variables/parameters

For pressure nozzles, it is well established that the atomization pressure will depend on a lot of parameters, including the liquid flowrate, the nozzle geometrical parameters and the solution physico-chemical properties. As the liquid flowrate is often imposed by the production to be achieved, the target parameter chosen here was *ΔP*, the difference between the pressure at the nozzle upstream and the one at the nozzle downstream (e.g. atmospheric pressure). The other variables to be considered can fall into 3 categories:

- Material-related variables: Fluid dynamic viscosity μ, fluid density ρ;
- Process-related variables: Volumetric flow rate $\dot{V}$;
- Nozzle geometry-related variables: see *Tab. 2a and 2b*.

Preliminary experiments showed no influence of the fluid surface tension over *ΔP*. This variable was thus not considered in this study. Knowing all the parameters susceptible to have a significant impact on *ΔP*, the general relation to identify can safely be expressed as *Eq. 1*:

$\Delta P = f(\mu, \rho, \dot{V}, w_s, d_s, l_s, n_s, d_b, d_o, d_m, l_o)$	*Eq. 1*

This "blind" equation can be rearranged and simplified by replacing some of the variables by hydrodynamically significant parameters. The hydrodynamic diameter d_h (*Eq. 2*) and the total section area of the slot A_s (*Eq. 3*) related to the slot geometry were therefore introduced to replace w_s, d_s and n_s:

$d_h = \frac{2.w_s.d_s}{w_s + d_s}$	*Eq. 2*

$A_s = n_s.w_s.d_s$	*Eq. 3*

By introducing these intermediate variables, we thus assume that w_s , d_s and n_s only have an impact through the parameters d_h and A_s, which was subsequently verified. Geometry parameters related to the orifice disc, d_o and d_m, can also be reinterpreted in terms of minimal section A_m and outlet section A_o (respectively *Eq. 4* and *5*):

$A_m = \pi.\frac{{d_m}^2}{4}$	*Eq. 4*

$A_o = \pi.\frac{{d_o}^2}{4}$	*Eq. 5*

When replacing these parameters in *Eq. 1*, we obtain the following simplified equation (*Eq. 6*):

$\Delta P = f(\mu, \rho, \dot{V}, d_h\ , A_s, l_s, d_b, A_o, A_m, l_o)$	*Eq. 6*

The values calculated for these new geometry parameters for the different nozzles considered are given in *Table 2*.

Table 2: Calculated nozzle geometry parameters

	1a	2b	3c	4d	1d	1b	1c	2a	2c	3a	4c
d_h (x10^{-3} m)	0.394	0.295	0.311	0.434	0.394	0.394	0.394	0.295	0.295	0.311	0.434
A_s (x10^{-6} m²)	0.623	0.370	0.670	1.134	0.623	0.623	0.623	0.370	0.370	0.670	1.134
A_o (x10^{-6} m²)	0.305	0.697	0.727	0.685	0.685	0.697	0.727	0.305	0.727	0.305	0.727
A_m (x10^{-6} m²)	0.207	0.215	0.275	0.316	0.316	0.215	0.275	0.207	0.275	0.207	0.275

3.2 Dimensions of the parameters

Three fundamental dimensions are involved in the parameters listed: the mass dimension M, the length dimension L and the time dimension T. Knowing this, it is possible to build a dimension matrix *D* containing, for each physical parameter (on the columns) the exponent of each fundamental dimension (on the lines) (*Tab. 3)*.

Table 3: Dimension matrix D, with central matrix C (dark grey) and Residual matrix R (white)

	ΔP	μ	d_h	l_s	d_b	A_o	A_m	l_o	ρ	A_s	$\dot{V}$
M	1	1	0	0	0	0	0	0	1	0	0
L	-1	-1	1	1	1	2	2	1	-3	2	3
T	-2	-1	0	0	0	0	0	0	0	0	-1

3.3 The Vashy-Buckingham theorem

The dimensional analysis procedure used involves the use of the Vashy-Buckingham theorem (Buckingham, 1914; Vashy, 1892). This theorem states that as *Eq. 6* expresses a relation *f* between 11 parameters depicted by 3 fundamental dimensions, it is possible to find a correlation *F* which relates (11-3) = 8 dimensionless numbers. However, it has to be noted that this theorem does not provide the form of the relationship between the dimensionless numbers.

3.4 Generation of the dimensionless numbers

3.4.1 Choice of a relevant repeated variables base

In order to generate the dimensionless relation *F* between all the parameters retained, the choice of a base, composed of repeated variables (opposed to the non-repeated variables, *i.e.* the variables not included in the base) is of prime importance. The variables of the base must be dimensionally independent, cover all the dimensions, and be of the number of fundamental dimensions (*i.e.* 3 here). It can be convenient to choose the base so that some of the dimensionless numbers generated (as for example those related to the target variable) have a precise physical meaning without having much recombination operations to perform afterwards. Especially, in the case of the atomization process, the discharge coefficient C_D was often used. The general expression for C_D is (*Eq. 7)*:

$$C_D = \frac{\dot{V}}{A_0.\sqrt{\frac{2.\Delta P}{\rho}}}$$	*Eq. 7*

However, in the case of hollow-cone nozzles, the nozzle outlet section A_0 may not be completely filled with the liquid due to the generation of an air core in the spray. C_D, as described by *Eq. 7,* is thus not recommended if a precise air core determination is not performed to allow the determination of the actual outlet section filled by the fluid. In Fluid Mechanics, it is also frequent to use the dimensionless Euler number *Eu,* defined as the ratio between the pressure forces and the inertial forces (Nonnenmacher and Piesche, 2000). *Eu* can be calculated in the studied geometry using *Eq. 8*:

$$Eu = \frac{\Delta P}{\rho.A_S^{-2}.\dot{V}^2}$$	*Eq. 8*

In order to easily make this number appear in the dimensionless relation *F*, $\{\rho, A_S, \dot{V}\}$ was chosen here as the base. The matrix defined in this base, highlighted in dark grey in *Table 3*, is called the central matrix (*C*) while the remaining matrix composed of the non-repeated variables is denoted the residual matrix (*R*).

3.4.2 Obtaining of the dimensionless numbers

Once the base chosen, the dimensionless numbers can be built by dividing each non-repeated variable by a product combination of the base variables. The purpose is then to find the adequate exponents *a*, *b* and *c* related to each of the base variables to ensure that, for each non-repeated variable, a dimensionless number *Π* arises with $\Pi = \frac{variable}{\rho^a.A_S^b.\dot{V}^c}$. The modified residual matrix *Rm* containing *a*, *b* and *c* values was obtained by Gaussian elimination (*Eq. 9*):

$Rm = C^{-1} \times R$	*Eq. 9*

The modified residual and central matrices arising are given in *Table 4.* Consequently, the dimensionless relation *F* is of the form depicted by *Eq. 10*.

Table 4: Modified residual Rm and central (in grey) matrices in the repeated variables base $\{\rho, A_s, \dot{V}\}$

	ΔP	μ	d_h	l_s	d_b	A_o	A_m	l_o	ρ	A_s	$\dot{V}$
a	1	1	0	0	0	0	0	0	1	0	0
b	-2	-0.5	0.5	0.5	0.5	1	1	0.5	0	1	0
c	2	1	0	0	0	0	0	0	0	0	1

$$Eu = \frac{\Delta P}{\rho . A_s^{-2} . \dot{V}^2} = F\left(\frac{\mu}{\rho . A_s^{-0.5} . \dot{V}}, \frac{d_h}{A_s^{0.5}}, \frac{d_b}{A_s^{0.5}}, \frac{l_s}{A_s^{0.5}}, \frac{A_o}{A_s}, \frac{A_m}{A_s}, \frac{l_o}{A_s^{0.5}}\right) \quad \textit{Eq. 10}$$

For concision concerns, the generated dimensionless numbers in *Eq. 10* will be noted Π_i with the *i* index corresponding to their position in *Eq. 9* (for example, $\Pi_2 = \frac{\mu}{\rho . A_s^{-0.5} . \dot{V}}$).

3.5 Reorganization of the dimensionless numbers and expression of the dimensionless function

The chosen base allowed the direct appearance of the *Eu* number as Π_1. Π_2 and Π_3 were also combined to make appear another physically relevant dimensionless number, the Reynolds number inside the distributor slots Re_s (*Eq. 11)*. Re_s was substituted to Π_2 in *F*.

$$Re_s = \frac{\rho . \dot{V} . d_h}{\mu . A_s} = \Pi_2^{-1} . \Pi_3 \quad \textit{Eq. 11}$$

By combining Π_3 and Π_5, a dimensionless number characterizing the nozzle geometry also appeared (*Eq. 12*) and was substituted to Π_5 in *F*:

$$\frac{l_s}{d_h} = \frac{A_s^{0.5}}{d_h} . \frac{l_s}{A_s^{0.5}} = \Pi_3^{-1} . \Pi_5 \quad \textit{Eq. 12}$$

Eq. 10 for *F* therefore turned into *Eq. 13* with 8 dimensionless numbers as stated by the theorem of Vashy-Buckingham:

$$Eu = \frac{\Delta P}{\rho . A_s^{-2} . \dot{V}^2} = F\left(Re_s, \frac{d_h}{A_s^{0.5}}, \frac{d_b}{A_s^{0.5}}, \frac{l_s}{d_h}, \frac{A_o}{A_s}, \frac{A_m}{A_s}, \frac{l_o}{A_s^{0.5}}\right) \quad \textit{Eq. 13}$$

At this stage of the dimensional analysis, it is mandatory to propose a mathematical form for the relation *F*. As proposed by several authors (Lallemand, 2000; *Scale-Up in Chemical Engineering*, 2006; Szirtes, 2007), it was assumed that a monomial relation is well suited to the analysis on a spraying process. According to *Eq. 13*, this monomial relation is presented in *Eq. 14,* where the coefficients a_0 to a_7 are constant. They will be identified from experimental measurements of ΔP in a wide range of conditions.

$$Eu = a_0 . (Re_s)^{a_1} . \left(\frac{d_h}{A_s^{0.5}}\right)^{a_2} . \left(\frac{d_b}{A_s^{0.5}}\right)^{a_3} . \left(\frac{l_s}{d_h}\right)^{a_4} . \left(\frac{A_o}{A_s}\right)^{a_5} . \left(\frac{A_m}{A_s}\right)^{a_6} . \left(\frac{l_o}{A_s^{0.5}}\right)^{a_7} \quad \textit{Eq. 14}$$

4. Results

4.1 Influence of the fluid properties, flow rate and nozzle geometry on ΔP

The evolution of the pressure drop ΔP in the nozzle was measured over the range of liquid flow rate available (up to 50 $L.h^{-1}$) changing the sprayed liquid (pure water or maltodextrin solutions) and the nozzle geometry (*Fig. 3a*). As expected, ΔP depends on the nozzle geometry and increases more or less rapidly with $\dot{V}$.

a.

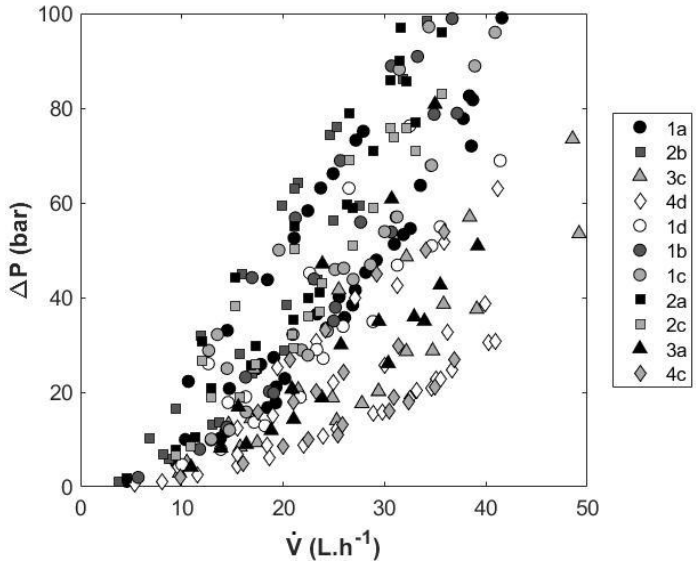

b.

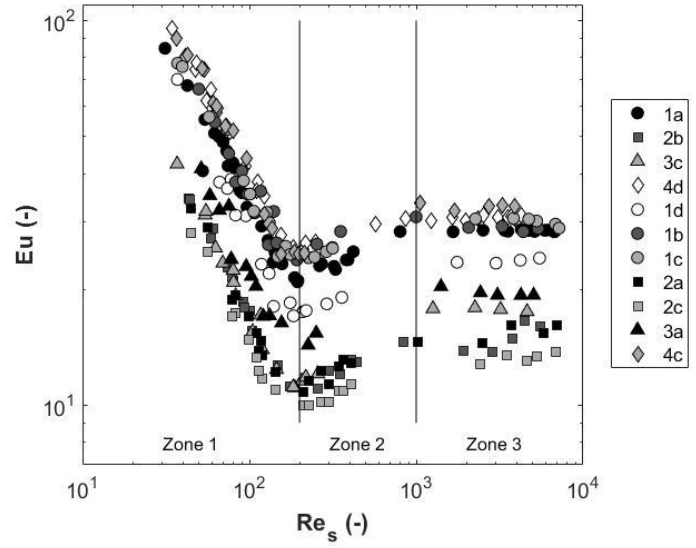

Figure 3: Evolution of the pressure drop in the nozzle (ΔP) measured changing the sprayed liquid (20°C) and the liquid flow rate for the different nozzle geometries in the dimensional space (ΔP vs. $\dot{V}$) (a); and in the dimensionless space (Eu vs. Re_s) (b).

As suggested by the dimensionless relation obtained (*Eq. 13*), experimental results can also be plotted in a dimensionless space *Eu* vs. Re_s (*Fig. 3b*). In this case, experiments conducted with the lowest viscosity products and highest volumetric flowrates correspond to the highest Re_s, while experiments performed with the most viscous solutions correspond to the lowest Re_s. As expected when considering *Eq. 14,* the trend observed for a specific nozzle is similar whatever the nozzle considered is, with an offset between the experimental data sets directly and solely related to the geometric parameters. Especially, for all the trends, two ruptures are observed at similar Re_s values, *i.e.* at Re_s about 200 and Re_s about 1000 respectively. This similarity allows the distinction between three different atomization zones depending on the Re_s value:

- Zone 1 for Re_s <200;
- Zone 2 for 200 <Re_s <1000;
- Zone 3 for Re_s > 1000.

It is noteworthy that, in Zone 3, the values obtained for *Eu* are independent of Re_s (therefore of the hydrodynamics in the throttle) and thus only depend on the geometry of the nozzle. Knowing that, a normalized Euler number *Eu** was introduced (*Eq. 15*):

$Eu^* = \frac{Eu}{\overline{Eu}}$	*Equation 15*

Where $\overline{Eu}$ is the mean value of *Eu* in Zone 3 for the corresponding nozzle geometry. When plotting the experimental data set in the new dimensionless space *Eu** vs. Re_s, they all fall into a single master curve, where the three zones previously identified still appear (*Fig. 4*). The use of *Eu** instead of *Eu*, thus allows to represent the impact of both the hydrodynamics and the geometry on a single curve. This validates that the offset observed in *Figure 3b* was actually due to the nozzle geometry and confirms the relevance of taking a monomial form for *F*. These results constitute a strong basis to propose ready-to-use relations for atomization set-up sizing when using swirl nozzles with throttled inlets.

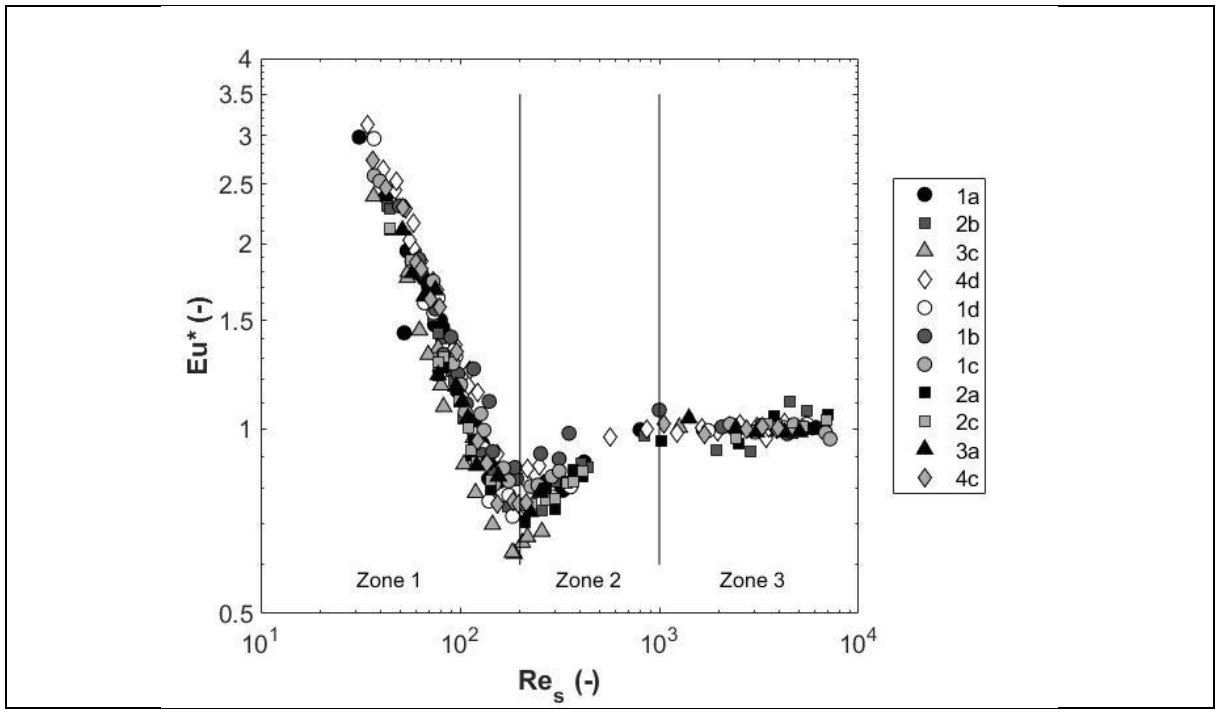

Figure 4: Experimental points represented in the dimensionless space Eu vs. Re_s*

4.2 Identification of coefficients of the dimensionless function

As it is confirmed that hydrodynamics have small or no influence on the *Eu* values obtained in Zone 3 and that the geometric parameters should be of the same influence independently on the zone considered, it was chosen to first identify the coefficients related to the geometry on the results obtained in Zone 3, and then to identify the ones related to Re_s on the measurements corresponding to the other zones. The relation to be identified in Zone 3 is thus (*Eq. 16*):

$$Eu = b_0.\left(\frac{d_h}{A_s^{0.5}}\right)^{b_1}.\left(\frac{d_b}{A_s^{0.5}}\right)^{b_2}.\left(\frac{l_s}{d_h}\right)^{b_3}.\left(\frac{A_o}{A_s}\right)^{b_4}.\left(\frac{A_m}{A_s}\right)^{b_5}.\left(\frac{l_o}{A_s^{0.5}}\right)^{b_6} \quad \textit{Eq. 16}$$

Through the multiple regression methodology mentioned in part *2.4*, the values of the seven b_i coefficients in *Eq. 16* were obtained with a correlation coefficient R^2=0.98. However, the corresponding p-values obtained with the statistical analysis showed that the coefficients b_1 and b_4 were not significant. *Eq. 16* was therefore simplified and an identification procedure on *Eq. 17* was performed. Values of the c_i coefficients and of the p-values obtained are presented in *Table 5*. The correlation coefficient R^2 was also equal to 0.98, confirming both the adequacy between the dimensionless relation obtained and the experimental data in Zone 3 and the small influence of the dimensionless numbers associated to b_1 and b_4.

$$Eu = c_0.\left(\frac{d_b}{A_s^{0.5}}\right)^{c_1}.\left(\frac{l_s}{d_h}\right)^{c_2}.\left(\frac{A_m}{A_s}\right)^{c_3}.\left(\frac{l_o}{A_s^{0.5}}\right)^{c_4} \quad \textit{Eq. 17}$$

Table 5: Values of coefficients c_i in Eq. 17 identified from experimental points in Zone 3 and corresponding p-values

	c_0	**c_1**	**c_2**	**c_3**	**c_4**
Value (-)	120.54	-1.88	0.47	-0.56	-0.09
p-value (-)	$3.29*10^{-30}$	$6.36*10^{-28}$	$8.18*10^{-22}$	$7.44*10^{-14}$	$2.75*10^{-5}$

The values of these coefficients identified in Zone 3 were then used to identify the rest of the coefficients for the two other zones. The dimensionless relations obtained for each of the three zones identified are presented in *Eq. 18*, *19* and *20.* The correlation coefficients obtained are, and R^2 = 0.96 for Zone 1, and R^2 = 0.94 for Zone 2, indicating that the monomial relations obtained give a fairly accurate description of the atomization phenomenon over the whole range of conditions studied.

Zone 1 $Re_s < 200$	$Eu = 6288.03.(Re_s)^{-0.82}$		*Eq. 18*
Zone 2 $200 < Re_s < 1000$	$Eu = 29.97.(Re_s)^{0.2}$	$\rightarrow .\left(\frac{d_b}{A_s^{0.5}}\right)^{-1.88}.\left(\frac{l_s}{d_h}\right)^{0.47}.\left(\frac{A_m}{A_s}\right)^{-0.56}.\left(\frac{l_o}{A_s^{0.5}}\right)^{-0.09}$	*Eq. 19*
Zone 3 $Re_s > 1000$	$Eu = 120.54$		*Eq. 20*

5. Discussion

5.1 Validity of the relations obtained

Eq. 18, *19* and *20* obtained from the experimental data set can strictly be applied in the data range where the measurements were performed (*Fig. 5)*. Another information useful for the experimenter is the deviation expected between the actual values and the theoretical ones estimated using these relations. When plotting the values actually measured against the ones estimated in the three Re_s zones (*Fig. 5*), almost all the values fall between the range ± 20%. *Figure 5* thus gives to the experimentalist willing to use the formula extrapolated in this study an operating diagram with a fairly comprehensive cartography of the accuracy and range of validity of the equations deduced.

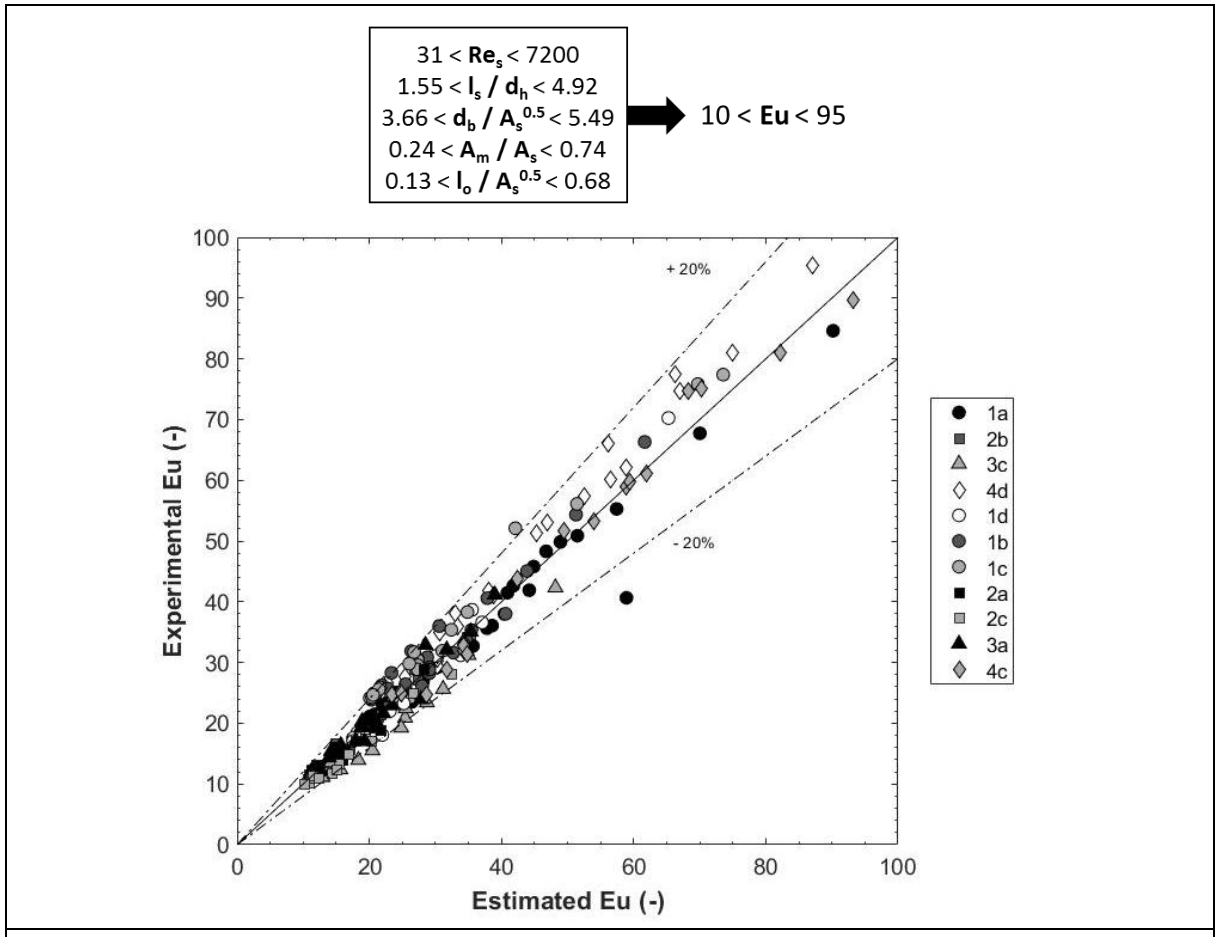

Figure 5: Operating diagram: Experimental Eu vs. estimated Eu values using Eq.18, 19 and 20 and validity domain of the correlations

5.2 Identification of the optimal spraying conditions

5.2.1 Spraying regimes

In the case of swirl nozzles, several authors observed and described the existence of different spraying regimes depending on the liquid flowrate (Ballester and Dopazo, 1996; Cousin et al., 1999;

Lefebvre and McDonell, 2017). These regimes were observed in the case of water spraying with the nozzle 4d, when progressively increasing the liquid flow rate to the maximal possible value (*Fig. 6*). At the lowest flowrates, the liquid tends to form a jet that fragments into large drops. The nozzle orifice is here completely filled with the liquid. As the flowrate is increased, the jet turns into an onion-shaped spray and then a tulip-spray. The droplets are getting finer and finer, the spray angle increases and the orifice section filled by the liquid is smaller and smaller. Ultimately, for the highest flowrates, a constant spray flowrate angle is obtained, and the length of the intact liquid sheet at the nozzle outlet decreases until turning invisible: this is the atomization regime. The orifice section filled by the liquid is then constant and at its lowest value. It has to be noted that a similar evolution was observed with all the nozzles considered in this study. These four regimes are consistent with the information that can be found in the literature.

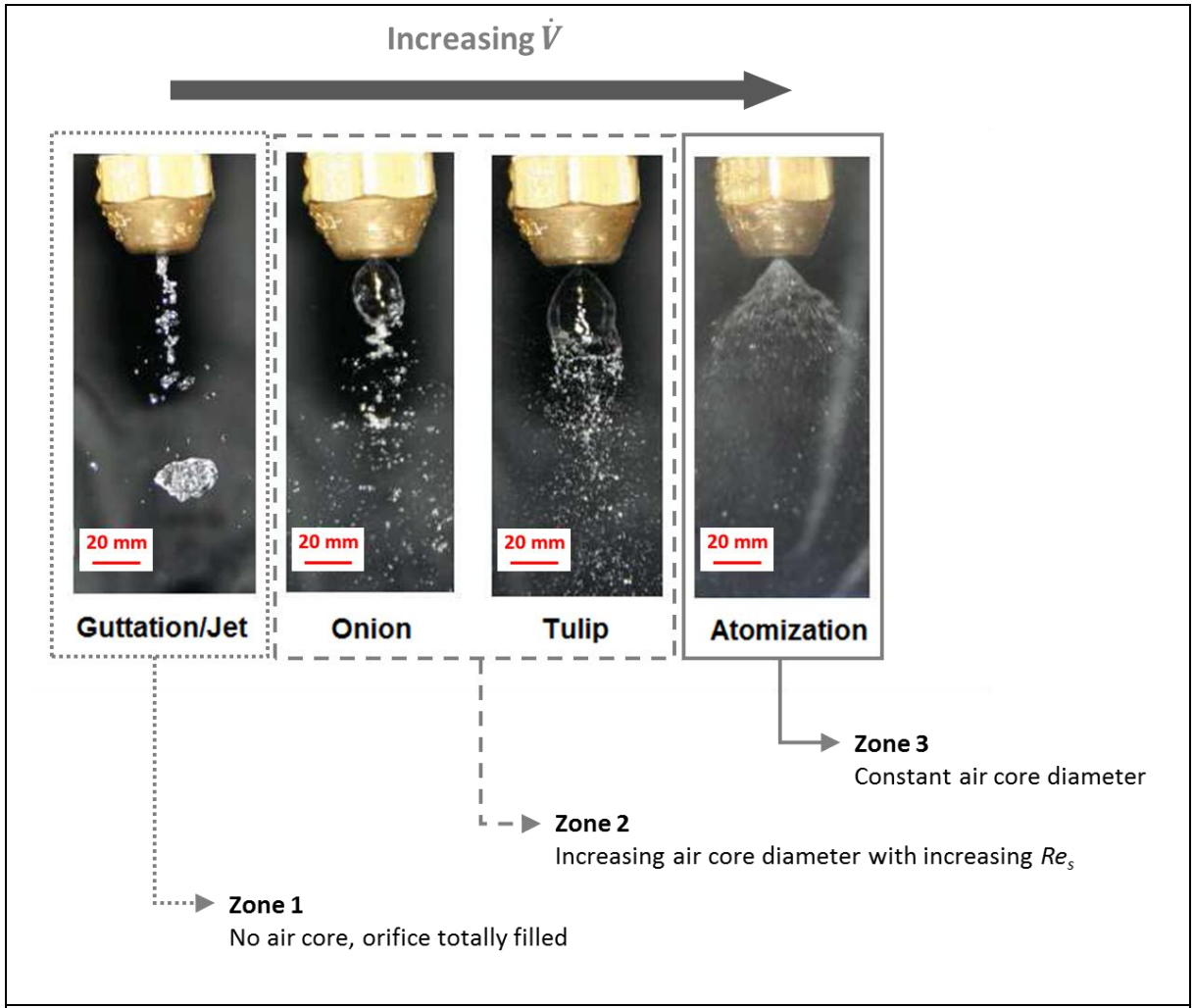

Figure 6: Spraying regimes observed when increasing the liquid flow rate (nozzle 4d, water at T=20°C)

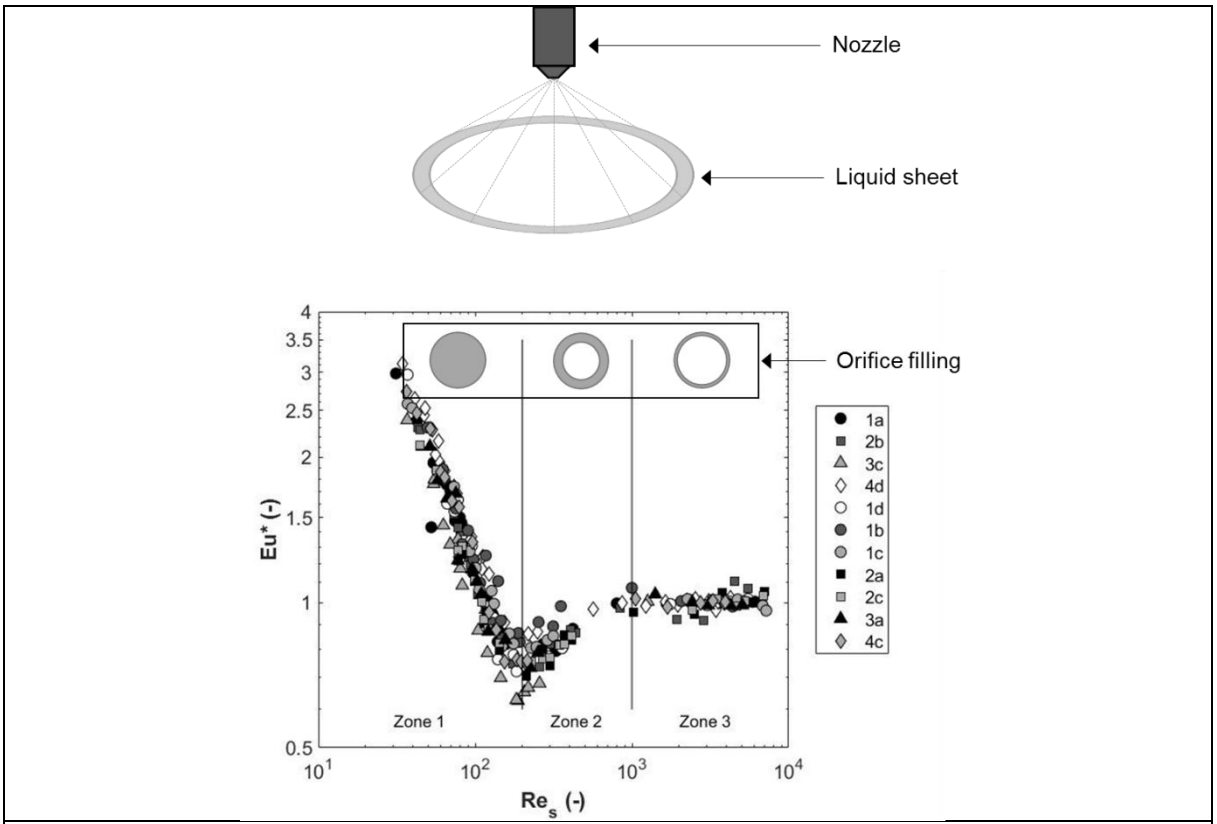

Figure 7: Atomization regimes and liquid sheet thickness

It is interesting here to relate these regimes, and the degree of filling of the orifice, to the three atomization zones identified through the dimensionless representation of our experimental data (*Fig. 7*). Actually, the evolution of the orifice filling is due to the generation of an air core when the value of the Reynolds number Re_s increases.

At low Reynolds number (Zone 1), the effect of the friction forces has a significant impact on the flow and, compared to the centrifugal forces in action inside the nozzle, they are too important to allow the development of an air core. This regime is to be avoided by all means since the viscous forces, compared to the other forces at stake, are too important and will not allow the generation of a spray. As a consequence, a decrease in the *Eu* value while increasing the Re_S was observed in Zone 1. This evolution was also reported in the literature by the means, for example, of the evolution of the discharge coefficient with increasing viscosity at constant spraying pressure (Bayvel and Orzechowski, 1993).

While increasing the Reynolds number, the centrifugal forces increasingly take over the friction forces up to a point in which the increase in the Reynolds number allows the generation of an air core of an increasing size: this is the regime observed in Zone 2. The existence of a range of Re_s values in which *Eu* is increasing before reaching a plateau was also reported in the literature for swirl nozzles, either by the through the evolution of *Eu* (Nonnenmacher and Piesche, 2000) or C_D (Halder et al., 2002; Lee et al., 2010). Anyway, in Zone 2, the onion-shaped and tulip shaped sprays give rise to liquid droplets with a coarse size distribution.

In Zone 3, the increase of the swirl is almost perfectly compensated by the resistance due to the friction forces at the outlet: the air core thus keeps a constant shape independently of the Reynolds value. This behavior in Zone 3, corresponding to the atomization regime, is very much recommended

for performing reliable atomization trials with minimal energy loss and narrow particle size distribution. The independency of *Eu* vs. Re_s at high Reynolds values was also confirmed in several studies with swirl nozzles (Halder et al., 2002; Chu et al., 2008; Datta and Som, 2000).

A similar overall behavior was already reported by Halder et al. (Halder et al., 2002) in the case of tangential inlet swirl atomizer. The authors also described the existence of two limiting Reynolds numbers: beyond the smaller one there is no air core initiation and above the larger one, the air core reaches a stable development. Despite the geometry studied by the above mentioned authors was different from the one studied in this paper, the physical underlying principles are similar and support the findings of the present study for axial inlet pressure swirl nozzles with throttle inserts.

5.2.2 Atomization regime and dimensionless function

As previously mentioned, Zone 3 is highly recommended when it comes to perform efficient liquid atomization. The main question arising thus concerns the conditions needed to reach this specific zone. Through the use of the dimensional analysis performed, it is possible to clearly quantify the minimal flowrate needed to reach this zone for a specified product and geometry. According to *Fig. 3*, the condition to reach Zone 3 entirely lies in the value of Re_s, that should be higher than 1000 (*Eq. 11* and *Eq.20*). If we call $\dot{V}_{min,zone\ 3}$ the minimal flowrate necessary to reach the atomization regime, we obtain the following relation (*Eq. 21*):

$\dot{V}_{min} = \frac{1000.\mu.A_s}{\rho.d_h}$	*Eq. 21*

Then, using *Eq. 13* and *Eq. 20*, it is possible to easily access the corresponding minimal pressure loss ΔP_{min} expected in atomization regime. *Table 5* shows some results obtained with solutions 1 and 2 and nozzles 1a, 2b, 3c, 4d. Similar calculations were also performed for zone 2 using Eq. 13 and Eq. 19.

Table 5: Minimal volumetric flowrate and corresponding spraying pressure to reach Zone 2 and 3

		Zone 2		Zone 3	
Solution	**Geometry**	$\dot{V}_{min}$ **(L.h^{-1})**	$\Delta P_{min,}$ **(bar)**	$\dot{V}_{min}$ **(L.h^{-1})**	$\Delta P_{min,}$ **(bar)**
1	1a	1.1	0.08	5.7	1.9
	2b	0.9	0.07	4.5	1.7
	3c	1.6	0.07	7.8	1.8
	4d	1.9	0.06	9.4	1.6
2	1a	20.7	27.6	103.5	689.7
	2b	16.4	25.2	82.1	630.9
	3c	28.2	26.8	141.0	669.1
	4d	34.2	23.4	171.0	586.0

The geometry has an obvious influence on the minimal flowrate needed to reach Zone 3, however the main point of vigilance lies in the fluid properties to be sprayed, especially the dynamic viscosity. While the density between solution 1 and 2 is almost similar (*Table 1*), the dynamic viscosity is 20 times higher for solution 2. This consequently multiplies the necessary flowrate to reach zone 3 by approximately 20, and thus the resulting pressure loss which is around 400 times higher. That means it is not possible to reach the Zone 3 with a 20 mPa.s viscosity solution with the pilot plant used in this study. For a moderately viscous fluid sprayed on these nozzles, depending on the pumping device capacity, atomization regime is thus not guaranteed. This fact legitimates the identification of *Eq. 19*, which can be of great use. Actually, the pressure loss to enter Zone 2 (between 20 and 30 bar for solution 2) is in that case in accordance with the capacity of the pilot plant used here. The corresponding minimum flow rate is also significantly smaller. Concerning Zone 1, according to our observations, the regime related to this zone does not correspond to an acceptable atomization.

5.2.3 Drying experiments

Beyond the identification of ideal spray conditions, it is also important to know their impact on the size distribution of the droplets generated. Especially, in the spray drying process, it has a great impact on the dry particle size distribution and on the final powder properties.

Whilst the measurement of the size distribution of the liquid drops generated at the nozzle outlet is not simple, the measurement of the size distribution of the particles obtained after spray drying maltodextrin solutions is relatively simple (laser granulometry).

Some spray drying trials were therefore performed to observe the impact of some parameters on the evolution of the final mean Sauter diameter of the powder (d_{32}). The dryer used was a TechniProcess SDF6 (evaporation capacity of 22 kg.h^{-1}). Atomization regime was visually assessed through a transparent wall. All the drying experiments were performed using the same conditions for drying air (flowrate 550 kg.h^{-1} with inlet and outlet temperature respectively equals to 180°C and 80°C). The mean Sauter diameter of the recovered powder was assessed through SLS measurements (MasterSizer 2000, Malvern Instruments, UK). Two nozzles (1a, 2b) and four MD DE 15 solutions with different concentration were spray dried modifying the liquid flowrate $\dot{m}$ in order to cover Re_s values between about 80 and 2000. The operating conditions (mass flowrate $\dot{m}$, Re_s value) and the obtained d_{32} values are presented in *Table 6*.

Table 6: Drying experiments performed using nozzles 1a, 2b and MD DE 15 solutions

Nozzle	MD concentration (kg/kg sol.)	μ (Pa.s)	$\dot{m}$ (kg.s^{-1})	Re_s (-)	Zone	d_{32} (µm)
1a	0.47	0.07	33.0	83	1	-
1a	0.35	0.02	24.6	216	2	69
2b	0.35	0.02	24.6	272	2	52
1a	0.25	0.004	21.2	931	2	52
1a	0.1	0.002	17.5	1555	3	39
2b	0.1	0.002	17.8	1971	3	30

Droplets generated at low Reynolds (Zone 1) were too big to be efficiently dried, resulting in no powder production. This behavior is in accordance with the previous description of atomization in Zone 1. For Re_s number higher than 200, at constant geometry, the effect of an increase in Re_s is

quite clear: the higher Re_s, the lower d_{32}. At constant flowrate and product, a change in geometry will induce a change in Re_s, and thus in powder size.
While deeper investigation has to be proceeded in order to give more insight of the influence of some parameters (particularly the surface tension) over the size distribution obtained after spraying and then after drying, these preliminary results give interesting hints of the influence of the hydrodynamics on the average size of the powder achievable with such nozzles.

Conclusion

Through the means of a comprehensive dimensional analysis methodology, this study overall provided a set of quantitative relations allowing the prediction of the spraying pressure as a function of the relevant fluid properties, process operating conditions and nozzle geometric parameters for axial inlet swirl nozzles with throttle inserts. The mathematical relations obtained describes the influence of hydrodynamics (through the Reynolds number inside the slots) and geometric parameters over the normalized Euler number, chosen to represent the target parameter (*i.e.* the spraying pressure).

To identify the coefficients of the model, an experimental campaign (264 trials) was led on a pilot-scale plant with solutions of maltodextrin DE 15 as model fluids exhibiting a Newtonian rheological behavior. Also, a full geometric characterization of different pressure swirl nozzles was done to have a comprehensive access to the relevant geometric properties of the nozzle (initially 7 parameters).

Three distinct spraying zones were identified. They mainly depend on the relative importance of the friction forces over the centrifugal ones. The zone above Re_s = 1000 corresponds to the full atomization zone, where the conversion of pressure to kinetic energy is almost total (meaning no influence of Re_s). The relations identified can be used to precisely determine the conditions needed (especially the minimal volumetric flowrate) to achieve efficient atomization (meaning entering Zone 3) and estimate the corresponding spraying pressure.

This study also shows the benefits of a rigorous dimensional analysis approach for problems where numerous parameters have to be taken into account, allowing to obtain dimensionless relations easily usable by the scientist. It is general enough to be accurate in a large range of process conditions, fluids and geometric parameters. Such an approach is also suited to predict the influence of the process, geometric and fluid parameters over other relevant atomization parameters, as for example a characteristic droplet size.

Acknowledgements

The authors would like to thank TechniProcess for funding the PhD grant of V. Pistre.

Notations

a_i	Constant (*i* from 0 to 7) (-)
A_o	Outlet section (m²)
A_m	Orifice minimal section (m²)
A_s	Total section of the slots (m²)
b_i	Constant (*i* from 0 to 6) (-)
c_i	Constant (*i* from 0 to 4) (-)
C_D	Discharge coefficient (-)
d_b	Distributor base diameter (m)
d_h	Slot hydrodynamic diameter (m)
d_m	Orifice minimal diameter (m)
d_o	Orifice outlet diameter (m)
d_s	Slot depth (m)
d_{32}	Mean Sauter diameter (m)
Eu	Euler number (-)
$\overline{Eu}$	Averaged Euler number on Zone 1
$Eu*$	Normalized Euler number (-)
l_o	Orifice length (m)
l_s	Slot length (m)
$\dot{m}$	Fluid mass flowrate ($kg.s^{-1}$)
n_s	Number of slots (-)
Re_s	Slot Reynolds number (-)
T	Temperature (K)
$\dot{V}$	Fluid volumetric flowrate ($m^3.s^{-1}$)
$\dot{V}_{min}$	Minimal volumetric flowrate ($m^3.s^{-1}$)
w_s	Slot width (m)

ΔP	Pressure loss induced by the nozzle (Pa)
ΔP_{min}	Minimal pressure loss expected (Pa)
$\dot{\gamma}$	Shear rate (s^{-1})
μ	Fluid dynamic viscosity (Pa.s)
Π_i	Dimensionless number i (-)
ρ	Fluid density ($kg.m^{-3}$)

References

Alidoost Dafsari, R., Lee, S., Vashahi, F., Lee, J., 2016. An experimental study on flow and spray characteristics of pressure swirl nozzle with variation of swirl chamber length. KSAE2016 conference paper, 118–123.

Ballester, J., Dopazo, C., 1996. Drop size measurements in heavy oil sprays from pressure-swirl nozzles. Atomization and Sprays 6, 377–408. https://doi.org/10.1615/AtomizSpr.v6.i4.10

Ballester, J., Dopazo, C., 1994. Discharge coefficient and spray angle measurements for small pressure-swirl nozzles. Atomization and sprays 4, 351–367.

Bayvel, L., Orzechowski, Z., 1993. Liquid atomization. Taylor&Francis, Washington.

Buckingham, E., 1914. On physically similar systems; illustrations of the use of dimensional equations. Physical Review 4, 345–376. https://doi.org/10.1103/PhysRev.4.345

Butler Ellis, M.C., Tuck, C.R., 1999. How adjuvants influence spray formation with different hydraulic nozzles. Crop Protection 18, 101–109. https://doi.org/10.1016/S0261-2194(98)00097-0
Chu, C.-C., Chou, S.-F., Lin, H.-I., Liann, Y.-H., 2008. An experimental investigation of swirl atomizer sprays. Heat and Mass Transfer 45, 11–22. https://doi.org/10.1007/s00231-008-0389-1
Cousin, J., Ren, W.M., Nally, S., 1999. Recent developments in simulations of internal flows in high pressure swirl injectors. Oil & Gas Science and Technology 54, 227–231. https://doi.org/10.2516/ogst:1999019
Datta, A., Som, S.K., 2000. Numerical prediction of air core diameter, coefficient of discharge and spray cone angle of a swirl spray pressure nozzle. International Journal of Heat and Fluid Flow 21, 412–419. https://doi.org/10.1016/S0142-727X(00)00003-5
Delaplace, G., Loubière, K., Ducept, F., Jeantet, R., 2015. Dimensional analysis of food processes, ISTE Press. ed. Elsevier.
Halder, M.R., Dash, S.K., Som, S.K., 2002. Initiation of air core in a simplex nozzle and the effects of operating and geometrical parameters on its shape and size. Experimental Thermal and Fluid Science 26, 871–878. https://doi.org/10.1016/S0894-1777(02)00153-X
Hoffmann, W.C., Fritz, B.K., Martin, D.E., 2011. Air and spray mixture temperature effects on atomization of agricultural sprays. Agricultural Engineering International: CIGR Journal 13.
Jain, M., John, B., Iyer, K.N., Prabhu, S.V., 2014. Characterization of the full cone pressure swirl spray nozzles for the nuclear reactor containment spray system. Nuclear Engineering and Design 273, 131–142. https://doi.org/10.1016/j.nucengdes.2014.02.025
Jones, A.R., 1982. Factors affecting the performance of large swirl pressure jet atomizers (CEGB Rep . R/M/N1054,). Marchwood, Southampton, UK.
Lallemand, A., 2000. Écoulement des fluides - Analyse dimensionnelle. Similitude. Techniques de l'Ingenieur 1–16.
Lee, E.J., Oh, S.Y., Kim, H.Y., James, S.C., Yoon, S.S., 2010. Measuring air core characteristics of a pressure-swirl atomizer via a transparent acrylic nozzle at various Reynolds numbers. Experimental Thermal and Fluid Science 34, 1475–1483. https://doi.org/10.1016/j.expthermflusci.2010.07.010
Lefebvre, A.H., McDonell, V.G., 2017. Atomization and sprays, Second edition. ed. CRC Press, Taylor & Francis, Boca Raton.
Mandato, S., Rondet, E., Delaplace, G., Barkouti, A., Galet, L., Accart, P., Ruiz, T., Cuq, B., 2012. Liquids' atomization with two different nozzles: Modeling of the effects of some processing and formulation conditions by dimensional analysis. Powder technology 224, 323–330.
Marchione, T., Allouis, C., Amoresano, A., Beretta, F., 2007. Experimental investigation of a pressure swirl atomizer spray. Journal of Propulsion and Power 23, 1096–1101. https://doi.org/10.2514/1.28513
McCreery, G.E., Stoots, C.M., 1996. Drop formation mechanisms and size distributions for spray plate nozzles. International Journal of Multiphase Flow 22, 431–452. https://doi.org/10.1016/0301-9322(95)00086-0
Moon, S., Abo-Serie, E., Bae, C., 2010. Liquid film thickness inside the high pressure swirl injectors: Real scale measurement and evaluation of analytical equations. Experimental Thermal and Fluid Science 34, 113–121. https://doi.org/10.1016/j.expthermflusci.2009.09.007
Moon, S., Abo-Serie, E., Bae, C., 2009. Air flow and pressure inside a pressure-swirl spray and their effects on spray development. Experimental Thermal and Fluid Science 33, 222–231. https://doi.org/10.1016/j.expthermflusci.2008.08.005
Nasr, G.G., Yule, A.J., Bendig, L., 2010. Industrial sprays and atomization: design, analysis and applications. Lightning Source UK Ltd., Milton Keynes UK.
Nonnenmacher, S., Piesche, M., 2000. Design of hollow cone pressure swirl nozzles to atomize Newtonian fluids. Chemical Engineering Science 55, 4339–4348. https://doi.org/10.1016/S0009-2509(00)00043-9
Rizk, N.K., Lefebvre, A.H., 1985. Internal flow characteristics of simplex swirl atomizers. Journal of Propulsion and Power 1, 193–199. https://doi.org/10.2514/3.22780

Scale-Up in Chemical Engineering, 2nd edition. ed, 2006. . Wiley-VCH Verlag GmbH & Co. KGaA, Weinheim, FRG. https://doi.org/10.1002/352760815X.fmatter
Szirtes, T., 2007. Applied dimensional analysis and modeling. Butterworth-Heinemann, Elsevier. https://doi.org/10.1016/B978-012370620-1.50005-8
Vashy, A., 1892. Sur les lois de similitude en physique. Annales Télégraphiques 19, 25–28.